Molecular Helicity in Inorganic Complexes; Bi- and Tri-nuclear Complexes of 2,2′:6′,2″:6″,2‴:6‴,2⁗:6⁗,2⁗′-Sexipyridine and the Crystal and Molecular Structure of Bis(μ-2,2′:6′,2″:6″,2‴:6‴,2⁗:6⁗,2⁗′-sexipyridine-κ^3*N,N′,N″*:κ^3*N‴,N⁗,N⁗′*)dicadmium Hexafluorophosphate–Acetonitrile (1/4)†

Edwin C. Constable,[*,a] **Michael D. Ward**[a] **and Derek A. Tocher**[*,b]
[a] *University Chemical Laboratory, Lensfield Road, Cambridge CB2 1EW, UK*
[b] *Department of Chemistry, University College London, 20 Gordon St., London WC1H 0AJ, UK*

The potentially sexidentate ligand 2,2′:6′,2″:6″,2‴:6‴,2⁗:6⁗,2⁗′-sexipyridine (L) has been prepared and shown to demonstrate considerable structural versatility in forming double helical binuclear complex cations of the type $[M_2L_2]^{4+}$ (M = Mn^{II}, Fe^{II}, Cu^{II} or Cd^{II}) or $[M_3L_2]^{3+}$ (M = Cu^{I} and Ag^{I}). A binuclear palladium(II) complex with a metal:ligand stoichiometry of 2:1 has also been characterised. The electrochemical properties of these complexes are reported, together with redox-initiated interconversions of $[Cu_3L_2]^{n+}$ and $[Cu_2L_2]^{n+}$ species. The crystal and molecular structure of the double helical complex $[Cd_2L_2][PF_6]_4\cdot$4MeCN [space group *C*2/*c*, *a* = 20.466(8), *b* = 18.872(6), *c* = 20.617(5) Å, β = 111.98(2)°, *R* = 0.0599, *R′* = 0.0634] is reported; the two metal centres are separated by 4.173(4) Å and coplanar pyridyl rings of the two independent ligands within the cation show short π-stacking interactions.

There has been considerable recent interest in the design of ligands that facilitate the spontaneous self-assembly of complexes[1] and host–guest compounds[2] with novel chemical, biological or topological properties. In particular, inorganic complexes containing a double helical geometry have been the focus of much attention, and we[3,4] and others[5] have demonstrated the formation of a variety of double helical complexes containing polypyridine ligands. The double helix is the basic building block which is utilised in the preparation of catenated and knotted molecules.[6] We have shown that the double helical ligand array arises when a conjugated polydentate ligand interacts with a metal ion that is too small for the bonding cavity that would occur in a *planar* ligand configuration, and have also observed that π-stacking interactions play an important role in stabilising the double helical geometry. We recently briefly reported the synthesis and X-ray crystal structure of a double helical dicadmium(II) complex of 2,2′:6′,2″:6″,2‴:6‴,2⁗:6⁗,2⁗′-sexipyridine (L),[4] and now report in detail the preparation, characterisation and some electrochemical and spectroscopic properties of complexes of L with a variety of first- and second-row transition metals.

Experimental

Infrared spectra were recorded on a Perkin-Elmer 1710 Fourier-transform spectrophotometer, with the samples in compressed KBr discs, proton NMR spectra on Brüker WM-250 or AM400 spectrometers. Fast atom bombardment (FAB) and electron impact (EI) mass spectra were recorded on a Kratos MS-50 spectrometer, with 3-nitrobenzyl alcohol as matrix for the FAB spectra. ESR spectra were recorded on a Varian E-109 spectrometer as frozen acetonitrile glasses at 90 K. Electrochemical measurements were performed using an AMEL model 553 potentiostat, model 567 function generator and model 721 integrator connected to an X-Y recorder *via* an AMEL model 560/A interface. A conventional three-electrode configuration was used, with platinum-bead working and auxiliary electrodes and an Ag–AgCl reference. Ferrocene was added at the end of each experiment as an internal standard. Controlled-potential electrolyses were performed using a cylindrical platinum gauze as working electrode and a smaller, coaxial, platinum gauze as auxiliary electrode (separated by a frit). The solvent was acetonitrile in all cases, distilled from CaH_2 and then P_4O_{10} and stored over 4 Å molecular sieve. The base electrolyte was 0.1 mol dm^{-3} $[NBu_4][BF_4]$, recrystallised twice from methanol–water. Potentials are quoted *vs.* ferrocene–ferrocenium couple (0.0 V), and all potentials were referenced to internal ferrocene added at the end of each experiment. 2,2′-Bipyridine, Karl-Fischer grade pyridine and other reagents were used as supplied (Aldrich or Fisons); 6,6′-diacetyl-2,2′-bipyridine,[7] 2-[1-oxo-3′-(1″-pyrrolidino)propyl]pyridinium ethanedioate[8] and $[Cu(MeCN)_4][PF_6]$[9] were prepared according to published procedures

Preparations.—*6,6′-Bis*(1-*pyridinioacetyl*)-2,2′-*bipyridine diiodide*. 6,6′-Diacetyl-2,2′-bipyridine (1.00 g, 4.16 mmol) was added to a solution of iodine (2.11 g, 8.33 mmol) in anhydrous pyridine (20 cm^3). The mixture was then heated to reflux for 1 h and then the dark coloured solution allowed to cool slowly to room temperature, when a yellow solid precipitated. This product was collected by filtration and washed with a small quantity of ice-cold methanol to yield 6,6′-bis(1-pyridinioacetyl)-2,2′-bipyridine diiodide as a yellow solid (2.16 g, 80%). FAB MS: *m*/*z* 523 (M^+ − I), 444 (M^+ − I − py), 395 (M^+ − 21) and 317 (M^+ − 2I − py) ^{1}H NMR (CD_3SOCD_3): δ 6.78 (4 H, s, CH_2), 8.23 (2 H, d, *J* 7.8, $H^{3,5}$), 8.37 (4 H, t, *J* 7.8, pyridinium H^3), 8.44 (2 H, t, *J* 7.8, H^4), 8.79 (2 H, t, *J* 7.8, pyridinium H^4), 9.07 (4 H, d, *J* 7.8, pyridinium $H^{2,6}$ and 9.10 (2 H, d, *J* 7.8 Hz, $H^{3,5}$ (Found: C, 44.1; H, 3.4; N, 8.4. Calc. for $C_{24}H_{20}I_2N_4O_2$: C, 44.3; H, 3.1; N, 8.6%).

---

† *Supplementary data available:* see Instructions for Authors, *J. Chem. Soc., Dalton Trans.*, 1991, Issue 1, pp. xviii–xxii.

Table 1 Partial microanalytical data for complexes of sexipyridine (L), with calculated values in parentheses

Complex	Analysis (%) C	H	N
$[Cu_3L_2][PF_6]_3$	46.6	2.6	11.0
	(46.4)	(2.6)	(10.8)
$[Cu_2L_2][PF_6]_4{\cdot}4H_2O$	41.4	2.9	10.2
	(42.2)	(2.8)	(9.8)
$[Mn_2L_2][PF_6]_4$	44.1	2.4	10.5
	(44.5)	(2.5)	(10.4)
$[Fe_2L_2][PF_6]_4{\cdot}H_2O$	43.6	2.6	10.0
	(44.0)	(2.6)	(10.3)
$[Cd_2L_2][PF_6]_4{\cdot}2H_2O$	39.9	2.2	9.4
	(40.7)	(2.5)	(9.5)
$[Ag_3L_2][PF_6]_3$	42.5	2.6	10.2
	(42.7)	(2.4)	(10.2)
$[Pd_2L(O_2CMe)_2][PF_6]_2{\cdot}MeCN$	38.7	2.6	8.8
	(38.4)	(2.6)	(8.7)

2,2′:6′,2″:6″,2‴:6‴,2⁗:6⁗,2⁗′-sexipyridine (L). A suspension of 2-[1-oxo-3′-(1″-pyrrolidino)propyl]pyridinium ethanedioate (0.91 g, 3.1 mmol), 6,6′-bis(1-pyridinioacetyl)-2,2′-bipyridine diiodide (1.00 g, 1.53 mmol) and ammonium acetate (4.0 g, excess) in aqueous methanol (1:1, 50 cm^3) was heated to reflux for 12 h. The crude solid product was collected by filtration and washed well with methanol. It was then added to toluene (100 cm^3), heated to reflux with a little activated charcoal for 10 min and then filtered hot through Celite. Concentration of the pale coloured filtrate *in vacuo* followed by cooling led to precipitation of 2,2′:6′,2″:6″,2‴:6‴,2⁗:6⁗,2⁗′-sexipyridine as a cream-coloured powder (0.114 g, 16%). EI MS: *m/z* 464 (M^+) (Found: C, 77.3; H, 4.1; N, 17.5. Calc. for $C_{30}H_{20}N_6$: C, 77.6; H, 4.3; N, 17.8%).

$[Cu_3L_2][PF_6]_3$. A suspension of L (0.093 g, 0.2 mmol) and $[Cu(MeCN)_4][PF_6]$ (0.112 g, 0.3 mmol) in methanol (20 cm^3) was heated to reflux for 2 h and then allowed to cool. The brown solid which precipitated was collected by filtration, washed well with methanol and recrystallised by the diffusion of diethyl ether vapour into an acetonitrile solution to yield dark brown microcrystals. Analytical data for this compound are presented in Table 1.

$[M_2L_2][PF_6]_4$ (M = Mn, Fe, Cu *or* Cd), $[Pd_2L(O_2CMe)_2][PF_6]_2$ *and* $[Ag_3L_2][PF_6]_3$. A suspension of L (0.093 g, 0.2 mmol) and a stoichiometric amount of the appropriate metal acetate (or chloride for M = Fe) in methanol was heated to reflux or sonicated until a clear solution was obtained. Addition of ammonium hexafluorophosphate precipitated the complexes, which were collected by filtration and recrystallised by the diffusion of diethyl ether vapour into an acetonitrile solution. Analytical data for these compounds is presented in Table 1.

Crystal Structure Determination of $[Cd_2L_2][PF_6]_4{\cdot}4MeCN$.—Single crystals of $[Cd_2L_2][PF_6]_4{\cdot}4MeCN$ were obtained as pale yellow needles by diffusion of diethyl ether vapour into an acetonitrile solution of the complex.

Crystal data. $C_{68}H_{52}Cd_2F_{24}N_{16}P_4$, $M = 1897.99$, monoclinic, space group *C*2/*c*, $a = 20.466(8)$, $b = 18.872(6)$, $c = 20.617(5)$ Å, $\beta = 111.98(2)°$, $U = 7384$ Å^3, $F(000) = 3776$, $Z = 4$, D_m not measured, $D_c = 1.71$ g cm^{-3}, Mo-Kα radiation ($\lambda = 0.710\ 73$ Å), μ(Mo-Kα) = 7.7 cm^{-1}, $T = 19$ °C.

Data collection and processing. A suitable pale yellow crystal of size 0.28 × 0.26 × 0.70 mm was mounted in a glass capillary tube with a fraction of the solvent from which it was crystallised. All geometric and intensity data were taken from this crystal using an automated four-circle diffractometer (Nicolet R3m/V). The lattice vectors were identified by application of the automatic indexing routine of the diffractometer to the positions of 29 reflections ($17 \leqslant 2\theta \leqslant 27°$) taken from a rotation photograph and centred by the diffractometer. Axial photography was used to verify Laue class and unit-cell dimensions. The ω–2θ technique was used to measure 7732 reflections (6512 unique) in the range $5 \leqslant 2\theta \leqslant 50°$. Three standard reflections were remeasured every 97 scans and showed no significant loss in intensity during the data collection. The data were corrected for intensity and polarisation effects and an empirical absorption correction applied. There are 3968 unique reflections with $I \geqslant 3\sigma(I)$. The data were solved in the monoclinic space group *C*2/*c*.

Structue analysis and refinement. The asymmetric unit contains one half of the binuclear cation, two $[PF_6]^-$ anions and two molecules of acetonitrile. The position of the unique cadmium atom was obtained by direct methods. The remaining non-hydrogen atoms were located by iterative least-squares refinement and Fourier difference syntheses. All non-hydrogen atoms of the cations and anions were refined anisotropically. The hydrogen atoms of the cation were included in idealised positions with a fixed isotropic thermal parameter, $U = 0.08$ Å^2. One of the solvent molecules occupies a general position within the asymmetric unit. The other, however, is disordered over the inversion centre, at (1,0,0) and the two-fold axis, at (1,*y*,0.25). A model was refined in which each site is occupied 50% of the time. Surprisingly it is the carbon atom of the methyl group which occupies the special positions. The occupancy of the two sites is not random throughout the crystal, as this would lead to some unreasonably short contacts between acetonitrile molecules in adjacent sites. The channels formed in the crystal because of this arrangement of lattice solvent molecules provide a facile route for loss of acetonitrile from the crystal, and explain the rapid loss of crystallinity observed on removing the crystalline material from the solvent in which it was recrystallised. The carbon and nitrogen atoms of these molecules were refined isotropically. The final least-squares refinement included 491 parameters for 3968 variables. The last cycle gave $R = 0.0599$, $R' = 0.0634$, weighting scheme $w^{-1} = \sigma^2(F) + 0.000\ 559\ F^2$ quality of fit 2.06, and did not shift any parameter by more than 0.012 times its estimated standard deviation (e.s.d.) The final Fourier difference map contained only a single peak above 1 e Å^{-3} (1.3 e Å^{-3} close to one of the $[PF_6]^-$ anions) but was otherwise featureless. Structure solution using SHELXTL+ on a Microvax II computer.[10] Atomic coordinates are presented in Table 2 and selected bond lengths and angles in Table 3.

Additional material available from the Cambridge Crystallographic Data Centre comprises H-Atom coordinates, thermal parameters and remaining bond lengths and angles.

Results and Discussion

The ligand 2,2′:6′,2″:6″,2‴:6‴,2⁗:6⁗,2⁗′-sexipyridine (L) was prepared by the Krohnke pyridine synthesis[11] as shown in Scheme 1. The procedure is very similar in essence to the known synthesis of 2,2′:6′,2″:6″,2‴:6‴,2⁗-quinquepyridine, except that 6,6′-diacetyl-2,2′-bipyridine[7] is used as the diketone instead of 2,6-diacetylpyridine. The terminal pyridine rings (rings A and F) originate from a 2-acetylpyridine derivative. Rings B and E are formed in the course of the synthesis by condensation of an enolate equivalent with an enone equivalent. The two central rings (C and D) originate in a 2,2′-bipyridine derivative. The reaction of 6,6′-diacetyl-2,2′-bipyridine (prepared from 2,6-dibromopyridine *via* 6,6′-dibromo-2,2′-bipyridine)[7] with iodine in pyridine results in the formation of a 'pyridacylpyridinium' salt, 6,6′-bis(1-pyridinioacetyl)-2,2′-bipyridine diiodide, which is a synthetic equivalent to the bisenolate of the diacetyl compound. This yellow salt was fully characterised on the basis of elemental analysis, ^1H NMR and mass spectroscopy. The Mannich base 2-[1-oxo-3′-(1″-pyrrolidino)propyl]pyridine cannot be prepared directly by the reaction of 2-acetylpyridine with pyrrolidine in the presence of formaldehyde, but may be obtained indirectly from the reaction of 2-lithiopyridine (generated *in situ* from 2-bromopyridine and *n*-

Table 2 Atomic coordinates for $[Cd_2L_2][PF_6]_4\cdot 4MeCN$

Atom	*x*	*y*	*z*
Cd(1)	1 070(1)	4 119(1)	2 666(1)
N(1)	−1 998(4)	4 297(4)	1 263(4)
N(2)	−1 248(3)	5 315(3)	2 128(4)
N(3)	−192(3)	4 786(3)	3 236(3)
N(4)	565(3)	3 429(3)	3 323(3)
N(5)	1 146(3)	2 932(3)	2 446(4)
N(6)	1 635(4)	3 973(3)	1 868(4)
C(1)	−2 364(5)	3 780(6)	858(5)
C(2)	−2 908(6)	3 899(6)	237(6)
C(3)	−3 089(6)	4 555(7)	26(6)
C(4)	−2 739(5)	5 112(6)	433(6)
C(5)	−2 187(4)	4 973(5)	1 067(5)
C(6)	−1 761(5)	5 532(5)	1 541(5)
C(7)	−1 873(6)	6 253(5)	1 393(5)
C(8)	−1 451(6)	6 729(5)	1 857(6)
C(9)	−921(6)	6 507(5)	2 447(6)
C(10)	−834(4)	5 785(4)	2 580(5)
C(11)	−296(4)	5 490(4)	3 224(5)
C(12)	70(5)	5 909(5)	3 789(5)
C(13)	539(5)	5 596(6)	4 383(6)
C(14)	639(5)	4 887(5)	4 411(5)
C(15)	272(4)	4 488(4)	3 832(4)
C(16)	358(4)	3 703(4)	3 825(4)
C(17)	251(5)	3 291(5)	4 334(5)
C(18)	350(5)	2 562(5)	4 308(5)
C(19)	562(5)	2 288(5)	3 803(5)
C(20)	666(4)	2 733(4)	3 311(4)
C(21)	918(4)	2 456(4)	2 776(4)
C(22)	932(5)	1 744(5)	2 637(6)
C(23)	1 187(5)	1 536(5)	2 149(6)
C(24)	1 421(5)	2 028(5)	1 791(5)
C(25)	1 407(5)	2 742(5)	1 957(5)
C(26)	1 670(5)	3 317(5)	1 648(5)
C(27)	1 972(6)	3 200(6)	1 149(6)
C(28)	2 230(6)	3 747(7)	900(6)
C(29)	2 201(6)	4 415(6)	1 140(6)
C(30)	1 884(5)	4 514(6)	1 614(5)
P(1)	4 117(2)	3 059(2)	591(2)
F(1)	4 545(5)	2 767(5)	1 335(4)
F(2)	3 701(6)	3 333(4)	−164(4)
F(3)	4 318(5)	2 398(5)	257(5)
F(4)	3 912(6)	3 724(6)	868(6)
F(5)	3 455(5)	2 661(7)	539(5)
F(6)	4 816(5)	3 432(6)	638(7)
P(2)	6 967(2)	1 666(2)	1 144(2)
F(7)	7 361(5)	2 266(5)	1 623(6)
F(8)	6 867(7)	2 057(8)	496(6)
F(9)	6 572(6)	1 075(5)	692(7)
F(10)	7 038(6)	1 274(6)	1 837(5)
F(11)	6 261(4)	1 988(7)	1 074(6)
F(12)	7 646(5)	1 298(8)	1 234(5)
N(7)	6 591(8)	4 776(8)	1 789(7)
C(31)	6 502(8)	4 216(10)	1 870(8)
C(32)	6 393(11)	3 491(12)	1 962(11)
N(8A)	9 828(11)	553(12)	1 061(12)
C(33A)	9 954(16)	291(16)	541(16)
C(34A)	10 000	0	0
N(8B)	9 676(12)	362(12)	1 597(13)
C(33B)	9 817(18)	−144(18)	2 098(17)
C(34B)	10 000	−626(16)	2 500

Table 3 Selected bond lengths (Å) and angles (°) for $[Cd_2L_2][PF_6]_4\cdot 4MeCN$

Cd(1)–N(4)	2.376(8)	Cd(1)–N(5)	2.301(7)
Cd(1)–N(6)	2.355(9)	Cd(1)–N(1A)	2.335(6)
Cd(1)–N(2A)	2.301(6)	Cd(1)–N(3A)	2.403(6)
N(4)–Cd(1)–N(5)	69.8(3)	N(4)–Cd(1)–N(6)	140.1(2)
N(5)–Cd(1)–N(6)	70.3(3)	N(4)–Cd(1)–N(1A)	85.1(2)
N(1A)–Cd(1)–N(5)	103.7(2)	N(1A)–Cd(1)–N(6)	103.8(3)
N(4)–Cd(1)–N(2A)	120.3(3)	N(5)–Cd(1)–N(2A)	166.8(3)
N(6)–Cd(1)–N(2A)	99.1(3)	N(1A)–Cd(1)–N(2A)	70.6(2)
N(4)–Cd(1)–N(3A)	111.7(2)	N(5)–Cd(1)–N(3A)	116.3(2)
N(6)–Cd(1)–N(3A)	88.6(3)	N(1A)–Cd(1)–N(3A)	139.8(2)
N(2A)–Cd(1)–N(3A)	69.5(2)	N(4)–Cd(1)–N(6)	140.1(2)

butyllithium) and 1-(2-ethoxycarbonylethyl)pyrrolidine (which is the addition product of ethyl acrylate and pyrrolidine). This Mannich base is most conveniently handled as the insoluble oxalate salt.[8] The reaction of the Mannich salt with 6,6′-bis(1-pyridinioacetyl)-2,2′-bipyridine diiodide proceeds smoothly in the presence of ammonium acetate to yield a dark coloured insoluble product. This crude product may be recrystallised from toluene to yield the desired ligand L as a pale cream solid in low yield. The new ligand is slightly soluble in benzene and toluene, but essentially insoluble in other organic solvents. Although it was possible to obtain solutions in CF_3CO_2H and CF_3CO_2D, the ^1H NMR spectra of such solutions were extremely broad, consistent with rapid deuterium exchange between the various possible protonated species. The EI mass spectrum of the compound exhibits a parent ion at *m*/*z* 464. A brief mention of $2,2':6',2'':6'',2''':6''',2'''':6'''',2'''''$-sexipyridine was made by Burstall[12] in his pioneering paper on the higher oligopyridines, but we have found the Krohnke synthetic method to be preferable.

The reaction of L with manganese(II) acetate in hot methanol results in the formation of a yellow solution, from which a pale yellow solid may be obtained upon treatment with ammonium hexafluorophosphate. Recrystallisation of this material from acetonitrile by the diffusion of diethyl ether vapour into the solution resulted in the deposition of analytically pure crystals of a compound which rapidly crumbled to a powder upon removal from the mother-liquor. Microanalysis suggested a stoichiometry $MnL(PF_6)_2$ for this material. The FAB mass spectrum showed peaks at *m*/*z* 1473, 1328, 1183, 664, 538 and 519 corresponding to the species $([Mn_2L_2][PF_6]_3)^+$, $([Mn_2L_2][PF_6]_2)^+$ and $([Mn_2L_2][PF_6])^+$, $([MnL][PF_6])^+$,

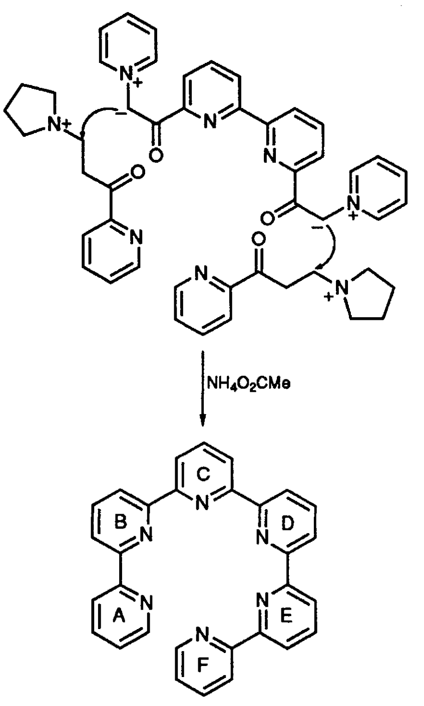

Scheme 1

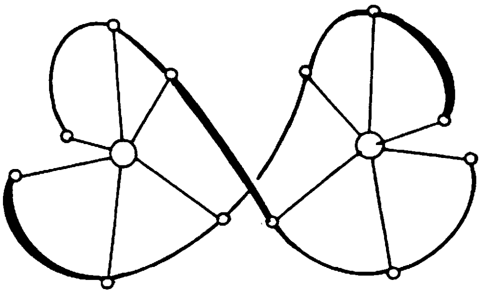

Fig. 1 Schematic representation of a binuclear double helical complex of L containing two six-co-ordinate metal centres

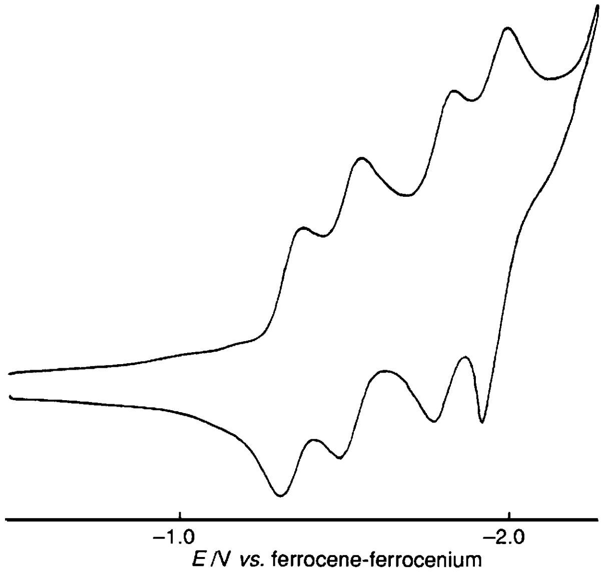

Fig. 2 Cyclic voltammogram of $[Mn_2L_2][PF_6]_4$

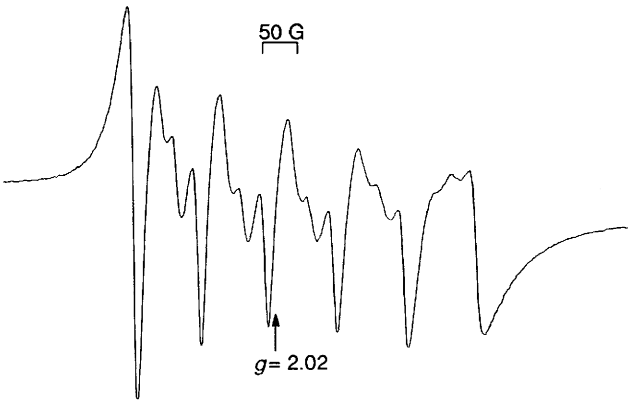

Fig. 3 ESR spectrum of an acetonitrile glass containing $[Mn_2L_2][PF_6]_4$

$[MnL(F)]^+$ and $[MnL]^+$ respectively. This, with the elemental analysis, suggests the formulation $[Mn_2L_2][PF_6]_4$ for the complex to be correct. This compound is expected to possess a double helical structure with each manganese(II) centre in a six-co-ordinate environment in which it is co-ordinated to a terdentate 'terpyridyl' portion of each of two L ligands (Fig. 1).

The complex is electrochemically active, and the cyclic voltammogram of an acetonitrile solution of the complex is shown in Fig. 2. No oxidation processes are observed to the limit of the solvent window (+1.4 V *vs.* ferrocene–ferrocenium). There are four well separated reductions, centred at $E_{\frac{1}{2}} = -1.34$, -1.52, -1.80 and -1.96 V. The first three are reversible one-electron processes (ΔE_p = 60–65 mV at all scan rates, and $i_{p_a} = i_{p_c}$). The return wave of the fourth reduction is obscured by an absorption process, and its precise nature is not apparent from the voltammogram. The absence of an oxidation wave is somewhat surprising, since the analogous mononuclear complexes oxidise readily; $[Mn(terpy)_2]^{2+}$ (terpy = 2,2′:6′,2″-terpyridine) exhibits a reversible Mn^{II}–Mn^{III} oxidation at +0.93 V.[13,*] The related complexes with bidentate ligands $[Mn(bipy)_3]^{2+}$ (bipy = 2,2′-bipyridine) and $[Mn(phen)_3]^{2+}$ (phen = 1,10-phenanthroline) show similar oxidations, but these are irreversible due to formation of mixed-valence manganese(III),(IV) dimers.[14] It thus appears that the manganese(II) centres in $[Mn_2L_2][PF_6]_4$ are stabilised with respect to oxidation by at least 500 mV relative to these mononuclear analogues. This we believe to be due to an electrostatic destabilisation of the higher oxidation states due to the close proximity of the two manganese(II) centres, although we cannot eliminate the possibility of a dramatically different geometry for the complexes in higher oxidation states. In contrast, the reductive processes observed for $[Mn_2L_2][PF_6]_4$ are consistent with those observed for the mononuclear complexes; $[Mn(terpy)_2]^{2+}$ undergoes two reversible one-electron reductions, at −1.47 and −1.81 V.[13] These were formally described as Mn^{II}–Mn^{I} and Mn^{I}–Mn^{0} processes, but no supportive evidence was given for this, and it is quite possible that one or both of the reductions are ligand-based. Attempts to perform bulk reductions of the $[Mn_2L_2][PF_6]_4$ solutions were unsuccessful; over the preparative time-scale, attempted reduction at a platinum gauze at potentials from −1.34 to −1.96 V led to the deposition of a yellow insoluble material upon the electrode.

We considered that there might be strong magnetic interactions between the two manganese(II) centres in $[Mn_2L_2][PF_6]_4$, which might provide an explanation for the anomalous oxidation behaviour of the complex. The ESR spectrum of $[Mn_2L_2][PF_6]_4$ in a frozen acetonitrile glass is shown in Fig. 3. The basic sextet at g 2.02 typical of high-spin manganese(II) ($S = \frac{5}{2}$) is apparent, but five of the six peaks are further split into triplets. The complexity of this signal strongly suggests an interaction between the two metal ions, since the mononuclear complexes $[Mn(terpy)_2]^{2+}$, $[Mn(bipy)_3]^{2+}$ and $[Mn(phen)_3]^{2+}$ all give simple sextets for their ESR spectra.[15] It is not satisfactory to suggest that the complexity of the spectrum results from the two metal ions being in different environments since this would give rise to only twelve lines in the spectrum (two overlapping sextets). It is also difficult to envisage a geometry for the complex in which the two manganese(II) centres are not equivalent (assuming that each is six-co-ordinate). A large zero-field splitting can cause extra lines to appear in manganese(II) ESR spectra,[16] but such behaviour is not apparent in $[Mn(terpy)_2]^{2+}$, $[Mn(bipy)_3]^{2+}$ or $[Mn(phen)_3]^{2+}$. The ESR spectra of $[Mn(terpy)_2]^{2+}$, $[Mn(bipy)_3]^{2+}$ or $[Mn(phen)_3]^{2+}$ do not exhibit any hyperfine coupling to ^{14}N, and it seems unlikely that this would be apparent for $[Mn_2L_2][PF_6]_4$.

The reaction of L with iron(II) chloride in warm methanol produces a deep red solution, from which a red solid is precipitated upon addition of ammonium hexafluorophosphate. Recrystallisation from acetonitrile by the diffusion of diethyl ether vapour into the solution yielded diamagnetic red needles, which lost solvent upon exposure to the air to give a red powder of stoichiometry $FeL(PF_6)_2$. The FAB mass spectrum of this material exhibited peaks at m/z 1475, 1330 and 1185 which may be assigned to $([Fe_2L_2][PF_6]_3)^+$, $([Fe_2L_2][PF_6]_2)^+$ and $([Fe_2L_2][PF_6])^+$ respectively. This, in combination with the elemental analysis, suggests that the complex should be formulated $[Fe_2L_2][PF_6]_4$, a double helical binuclear complex containing two six-co-ordinate iron(II) centres bonded to a terdentate 'terpyridyl' portion of each of two L ligands.

The complex is electrochemically active, and the cyclic

---

[*] The redox potentials quoted in this paper are actually *vs.* an Ag–AgCl reference and have been converted into the ferrocene–ferrocenium scale by subtracting 0.35 V.

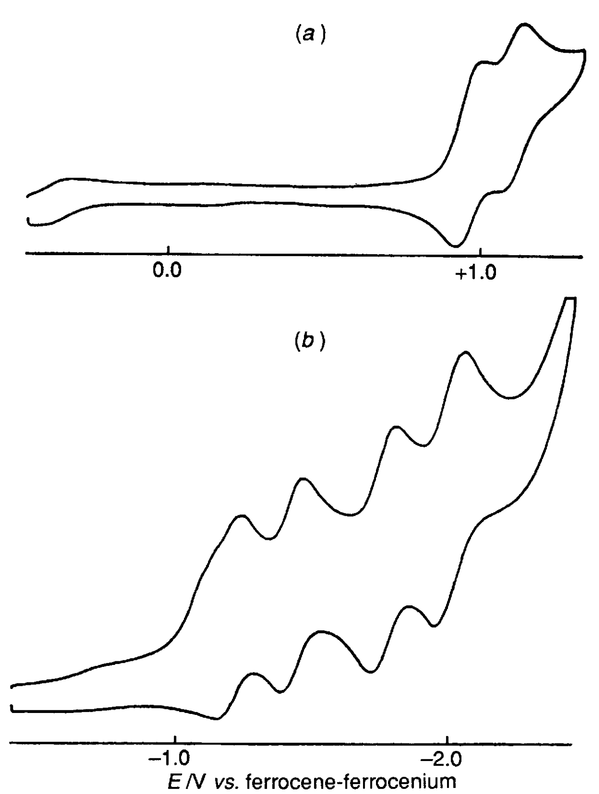

Fig. 4 Cyclic voltammogram of $[Fe_2L_2][PF_6]_4$ showing (*a*) oxidative and (*b*) reductive sweeps

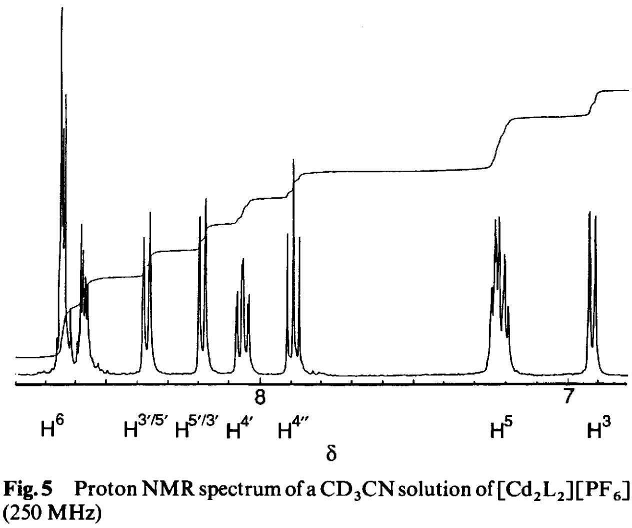

Fig. 5 Proton NMR spectrum of a CD_3CN solution of $[Cd_2L_2][PF_6]_4$ (250 MHz)

voltammogram of a solution of $[Fe_2L_2][PF_6]_4$ in acetonitrile is shown in Fig. 4. Two oxidation processes which correspond to formal $\{Fe^{II}–Fe^{II}/Fe^{III}–Fe^{II}\}$ and $\{Fe^{III}–Fe^{II}/Fe^{III}–Fe^{III}\}$ couples occur at +0.96 and +1.11 V. The oxidation centred at +0.96 V is fully reversible, whilst that at +1.11 V is quasi-reversible (ΔE_p = 75 mV at a scan rate of 100 mV s^{-1}). In contrast, $[Fe(terpy)_2]^{2+}$ exhibits an oxidation to the iron(III) state at +0.78 V.[13] Thus, the diiron(II) complex $[Fe_2L_2][PF_6]_4$ shows a similar resistance to oxidation compared to a mononuclear bis(2,2′:6′,2″-terpyridine) analogue as was observed for $[Mn_2L_2][PF_6]_4$, although in this case the stabilisation is not so marked. In this case there can be no magnetic interaction between the low-spin iron(II) centres, and the change in oxidation potential can be ascribed to either an electrostatic destabilisation of the 3+ oxidation state or to a distorted geometry in the helical complex. The bulk oxidation of an acetonitrile solution at a potential of +1.3 V resulted in the formation of a paramagnetic orange solution of the Fe^{III}_2 complex. The ESR spectrum of this species in an acetonitrile glass exhibited a broad near-isotropic signal centred at *g* 4.22. High-spin octahedral iron(III) complexes normally exhibit *g* values close to free spin in their ESR spectra,[17] but highly distorted six-co-ordinate environments are known to result in larger *g* values. A *g* value of 4.3 has been reported for a pyridine *N*-oxide complex[18] and one of 4.33 for the five-co-ordinate compound $[Fe(acac)_2Cl]$ (Hacac = pentane-2,4-dione).[19] The cyclic voltammogram of the complex $[Fe_2L_2][PF_6]_4$ also exhibits four reduction waves centred at $E_{\frac{1}{2}}$ = −1.17, −1.37, −1.67 and −1.98 V. The first three of these waves are fully reversible, whereas the fourth is quasi-reversible (ΔE_p = 80 mV at a scan rate of 100 mV s^{-1}). These values may be compared with those reported for $[Fe(terpy)_2]^{2+}$ which undergoes reversible reductions at −1.56 and −1.72 V;[13] it is not known whether these are metal- or ligand-based. The possibility of multiple ligand-based reductions at these potentials is well demonstrated by the electrochemistry of $[Zn_2(qpy)_2(O_2CMe)][PF_6]_3$ (qpy = 2,2′:6′,2″:6″,2‴:6‴,2⁗-quinquepyridine) which undergoes three reversible ligand-based reductions between −1.4 and −1.9 V.[20]

Pale yellow solutions were obtained upon heating L with methanolic solutions of cadmium(II) acetate, and the addition of ammonium hexafluorophosphate to these resulted in the deposition of a pale yellow solid. Recrystallisation of this solid from acetonitrile by the diffusion of diethyl ether vapour into a solution resulted in the deposition of yellow blocks or needles. These crystals lost solvent very readily upon removal from the solvent, and crumbled to a powder for which microanalysis indicated a formulation $CdL(PF_6)_2$. The FAB mass spectrum of this powder exhibited peaks at *m*/*z* 1587, 1442, 1297, 1040, 721 and 576 which may be assigned to the species $([Cd_2L_2][PF_6]_3)^+$, $([Cd_2L_2][PF_6]_2)^+$, $([Cd_2L_2][PF_6])^+$, $[CdL_2]^+$, $([CdL][PF_6])^+$ and $[CdL]^+$ (based upon ^{112}Cd, each species showing the correct isotopic distributions) respectively. Once again, the combination of FAB mass spectroscopic data with microanalytical results suggests that a binuclear formulation is appropriate. The complex is stable in solution, and the 250 MHz ^1H NMR spectrum of a CD_3CN solution is presented in Fig. 5. This clearly indicates that on the NMR time-scale the L ligands in the complex are equivalent and symmetrical about the interannular C–C bonds between rings C and D. This strongly supports the formation of a double helical binuclear complex in which the two cadmium centres are in similar six-co-ordinate environments in which they are bonded in a terdentate manner to a 'terpyridyl' donor set from each ligand. In order to confirm this proposal we have determined the crystal and molecular structure of the complex.

The X-ray crystal structure determination revealed the presence of acetonitrile molecules of solvation within the crystal lattice, and indicated that a formulation $[Cd_2L_2][PF_6]_4 \cdot 4MeCN$ was appropriate for the solvated complex. The cation is chiral, and both enantiomers are present equally within the crystal lattice. The crystal and molecular structure of one enantiomer of the complex cation $[Cd_2L_2]^{4+}$ together with the numbering scheme adopted) is shown in Fig. 6(*a*). A space-filling representation is in Fig. 6(*b*). The structural determination confirms the presence of the double helical binuclear cation. The two cadmium atoms are in identical six-co-ordinate environments, and are co-ordinated to three nitrogen atoms from a 'terpyridyl' group from each ligand. The two L ligands are crystallographically independent, and each cadmium interacts with three adjacent pyridine rings from each ligand. The cadmium–'terpyridyl' interactions with the two independent ligands differ slightly but significantly. The Cd–N bond lengths fall into the typical pattern observed for complexes of 2,2′,:6′,2″-terpyridine in which there are two longer [Cd(1)–N(6) 2.355(9), Cd(1)–N(4) 2.376(8), Cd(1)–N(1A) 2.335(6), Cd(1)–N(3A) 2.403(6) Å] and one shorter [Cd(1)–N(5) 2.301(7), Cd(1)–N(2A) 2.301(6) Å] metal–nitrogen contacts. The Cd–N distances are similar to, but slightly shorter than, those reported for the

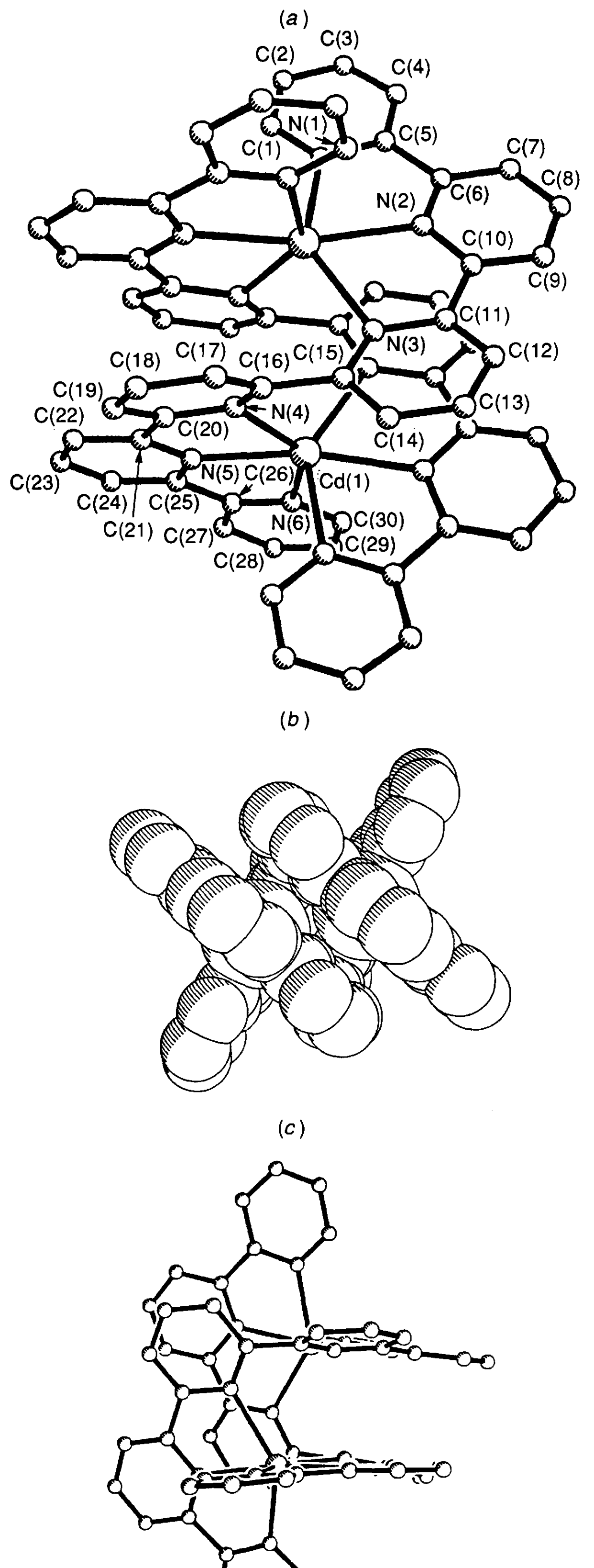

Fig. 6 (*a*) Crystal and molecular structure of one of the two enantiomers of the $[Cd_2L_2]^{4+}$ cation in $[Cd_2L_2][PF_6]_4 \cdot 4MeCN$ showing the numbering scheme adopted. Hydrogen atoms have been omitted for clarity. (*b*) An alternative space-filling representation of the $[Cd_2L_2]^{4+}$ cation emphasising the twisting within each ligand. (*c*) A view emphasising the stacking interactions within the cation

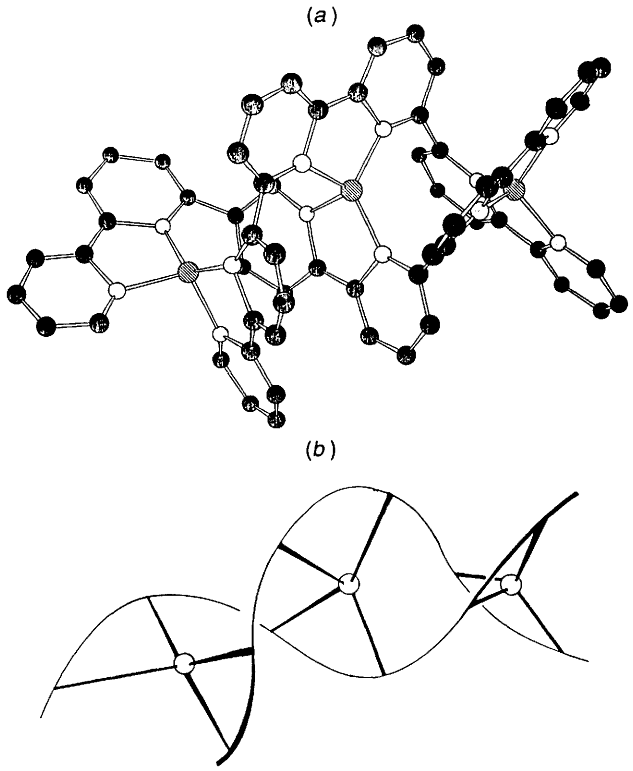

Fig. 7 Proposed structure (*a*) for the $[Cu_3L_2]^{3+}$ cation together with a schematic representation (*b*)

complex [Cd(terpy){Mn(CO)$_5$}$_2$] (Cd–N 2.475, 2.405, 2.493 Å).[21] The N–Cd–N angles are grossly distorted from those expected for an octahedral complex, or from those in a regular bis(2,2′:6′,2″-terpyridine) complex with molecular D_{2d} symmetry.[14] The metal–metal distance within the cation is 4.173(4) Å, which is considerably larger than twice the atomic radius (3.08 Å) and precludes any direct cadmium–cadmium interactions.

The double helical ligand array is formed by a series of twists about the interannular bonds within each of the ligands. The principal twist is of 57.3° between rings C and D [using a nomenclature with N(1) being in ring A, N(2) in ring B and so on], with considerably smaller twists of 2.0 (A–B), 12.1 (B–C), 13.2 (D–E) and 4.3° (E–F) at other sites contributing to the overall spiralling of the ligand. This is emphasised in Fig. 6(*b*). An approximately coplanar arrangement of the pyridine rings of the two ligands is a noticeable and important feature in the ligand array, and especially short contacts are observed for the symmetry-related pairs of rings B/C′ and C/B′ (3.736 Å, 170°) and D/E′ and E/D′ (3.561 Å, 171.9°). These interactions are emphasised in the projection shown in Fig. 6(*c*). No other interplanar contacts are below 4.0 Å. We have commented previously on the occurrence of these graphitic type π-stacking interactions within double helical ligand arrays.[3,4] There are no significant interactions between the hexafluorophosphate anions or the acetonitrile solvent molecules with the cations.

The reaction of L with a solution of [Cu(MeCN)$_4$][PF$_6$] in methanol produced a dark brown solid which was recrystallised from acetonitrile as diamagnetic dark brown blocks by the diffusion of diethyl ether vapour into the solution. The FAB mass spectrum of this material exhibited peaks at *m/z* 1407, 1262 and 1117, which may be assigned to $([Cu_3L_2][PF_6]_2)^+$, $([Cu_3L_2][PF_6])^+$ and $[Cu_3L_2]^+$ respectively (based on ^{63}Cu). The isotopic patterns of these peaks were consistent with these formulations, and were *not* consistent with dicopper products. Partial elemental analysis was also in accord with a formulation of the dark brown product as $[Cu_3L_2][PF_6]_3$. The proposed structure of this complex is given in Fig. 7. Molecular modelling

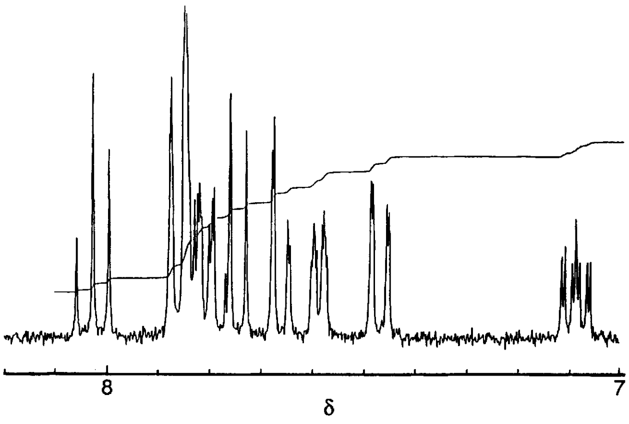

Fig. 8 Proton NMR spectrum of a CD_3CN solution of $[Cu_3L_2][PF_6]_3$ (250 MHz)

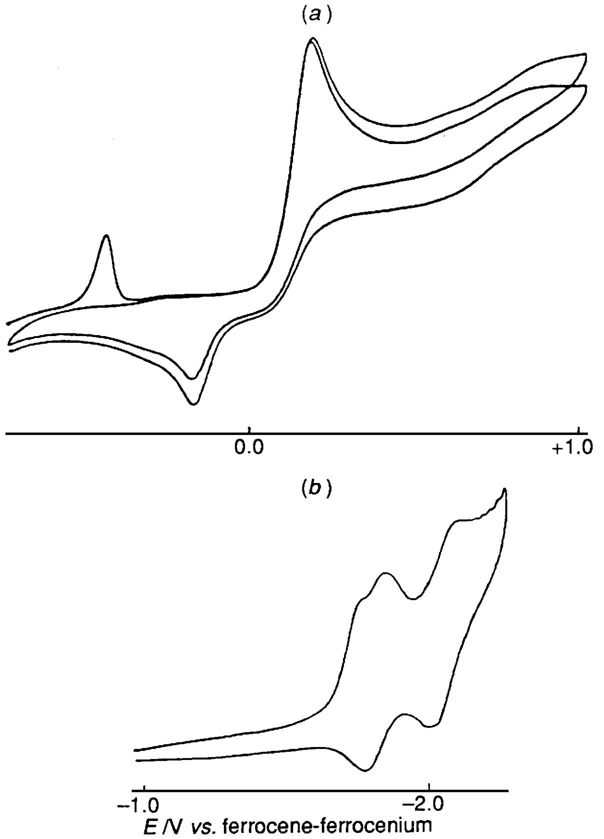

Fig. 9 Cyclic voltammogram of $[Cu_3L_2][PF_6]_3$ showing (*a*) oxidative and (*b*) reductive sweeps

studies indicate that it is just possible to fit three copper(I) ions inside the double helical array, albeit with somewhat distorted tetrahedral geometries. Each copper ion is four-co-ordinate, being attached to a pair of adjacent pyridyl residues from each L ligand in a distorted 'bis(2,2′-bipyridine)' environment. This linear arrangement of four-co-ordinate copper(I) ions along the helical backbone is reminiscent of the polynuclear helical complexes prepared by Lehn and other workers[5] from the interaction of copper(I) ions with flexible ligands containing a linear series of 2,2′-bipyridine subunits separated by aliphatic spacers. The ^1H NMR spectrum of a solution of $[Cu_3L_2][PF_6]_3$ (CD_3CN) is sharp and well resolved, and only ten proton environments are evident. This is consistent with a highly symmetrical D_2 average solution symmetry for the trinuclear cation.

In contrast to the above observations, the reaction of L with copper(II) acetate in methanolic solution resulted in the formation of clear, dark green, solutions from which a green solid was precipitated upon the addition of ammonium hexafluorophosphate. Recrystallisation of this from acetonitrile solution by the diffusion of diethyl ether vapour produced a mixture of green and brown microcrystals which could be separated manually. The brown material was identified as $[Cu_3L_2][PF_6]_3$ by FAB mass spectrometry. The green material showed peaks in the FAB mass spectrum at *m*/*z* 1489, 1344, 1199 and 1054 (based on ^{63}Cu), which correspond to $([Cu_2L_2][PF_6]_3)^+$, $([Cu_2L_2][PF_6]_2)^+$, $([Cu_2L_2][PF_6])^+$ and $[Cu_2L_2]^+$ respectively and are of the correct isotopic pattern for a *binuclear* copper species. The elemental analysis is also consistent with the formulation of the green material as $[Cu_2L_2][PF_6]_4$. The binuclear dicopper(II) complex presumably possesses a double helical geometry similar to those of the iron(II), manganese(II) and cadmium(II) complexes, although we cannot dismiss structures in which one or more pyridine rings are non-co-ordinated.

We have further investigated the nuclearity change in the double helical complex which is initiated by a redox change at the metal centre. A green acetonitrile solution of $[Cu_2L_2][PF_6]_4$ left in contact with air become dark brown over a period of a few days, and the resultant solution contained the trinuclear $[Cu_3L_2]^{3+}$ species. We have previously observed the reduction of copper(II) to copper(I) under aerobic conditions in other double helical complexes; the dicopper(II) complex $[Cu_2(qpy)_2(O_2CMe)][PF_6]_3$ reduces in solution to the mixed-valence complex $[Cu_2(qpy)_2][PF_6]_3$.[3]

The formation of both $[Cu_2L_2][PF_6]_4$ and $[Cu_3L_2][PF_6]_3$ underlines two characteristics of the double helical ligand array which we have also observed with the copper complexes of qpy;[3] the ligand array is flexible enough to adapt to the different geometric requirements of metal ions in different oxidation states [six- or five-co-ordinate for copper(II), four-co-ordinate for copper(I)], and also robust enough to maintain its integrity despite these changes. The interconversion of the forms is chemically reversible, and can be followed by electrochemistry.

The cyclic voltammogram of an acetonitrile solution of $[Cu_3L_2][PF_6]_3$ is shown in Fig. 9. There is an electrochemically irreversible oxidation centred at $+0.08$ V and a related irreversible reduction at -0.33 V. The controlled-potential oxidation of a sample of $[Cu_3L_2][PF_6]_3$ at a potential 200 mV more positive than the peak of the oxidation wave caused the dark brown solution to turn green, with formation of $[Cu_2L_2]^{4+}$. Coulometry indicated that the oxidation involved 2.1 ± 0.2 electrons per complex molecule, *i.e.* a two-electron oxidation. Thus, the copper ion ejected from the helical core is formally in oxidation state $+1$, although the possibility of fast electron transfer between the free copper ion and copper ions within the complex does not preclude other mechanistic possibilities. Although a copper ion was ejected during the oxidation, quantitative conversions of the trinuclear into the binuclear double helical complex were achieved. The ESR spectrum of the electrochemically generated $[Cu_2L_2]^{4+}$ was identical to that of chemically prepared $[Cu_2L_2][PF_6]_4$. It is unremarkable and consists of a broad, slightly asymmetric signal at $g = 2.08$ with a small hyperfine coupling to the copper nuclei just detectable. Re-reduction of the green solution obtained from the controlled-potential oxidation experiment at a potential 200 mV more negative than the reduction wave regenerated a brown solution, and involved transfer of the same amount of charge as required for the oxidation. The process is therefore fully *chemically* reversible, although electrochemically irreversible. In the tricopper(I) complex the three metal ions require a total of twelve donor atoms, which requirement may be satisfied by the double helical ligand array. Oxidation of one of the copper centres to the (II) oxidation state increases the co-ordination requirement to thirteen or fourteen donors. We have previously shown that such changes in overall oxidation state within a double helical ligand array results in changes in metal–metal distance and in the interannular twisting between

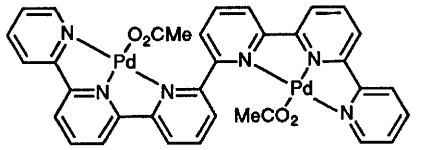

Fig. 10 Proposed structure for the complex $[Pd_2L(O_2CMe)_2][PF_6]_2$

pyridine rings. In the case of the complex cation $[Cu_3L_2]^{3+}$, it appears that the changes are such that the three metal centres cannot be accommodated.

The ligand L behaves with silver(I) ions in a similar manner to copper(I), and the reaction of L with silver(I) acetate in methanolic solution followed by treatment with ammonium hexafluorophosphate produced a yellow precipitate, which was recrystallised from acetonitrile–ether to yield a pale yellow microcrystalline solid. The FAB mass spectrum exhibited peaks at *m/z* 1537, 1430, 1392, 1285, 1140, 1033 and 569 (based on ^{107}Ag). These correspond to $([Ag_3L_2][PF_6]_2)^+$, $([Ag_2L_2][PF_6]_2)^+$, $([Ag_3L_2][PF_6])^+$, $([Ag_2L_2][PF_6])^+$, $[Ag_2L_2]^+$, $[AgL_2]^+$ and $[AgL]^+$. All of the isotopic patterns were consistent with these assignments. The presence of so many fragment ions is rather unusual, and perhaps indicates a fairly weakly bound complex, but these results do suggest the *trinuclear* formulation $[Ag_3L_2][PF_6]_3$. This is borne out by the elemental analysis, which exactly agrees with this formulation.

The core stoichiometry is thus the same as for the copper(I) complex, but molecular modelling studies indicate that the structures are unlikely to be the same. With a radius of approximately 1.3 Å, over 30% larger than copper(I), three silver(I) ions will not fit in a space that could only just accommodate three copper(I) ions. The Ag_3L_2 stoichiometry could be supported if one ligand is 'slipped' relative to the other, but we have no direct structural data to support this. The ^1H NMR spectrum of the complex is unhelpful, and only exhibits a series of broad, overlapping signals between δ 7 and 8.

The reaction of L with palladium(II) acetate in methanolic solution followed by treatment with ammonium hexafluorophosphate yielded a brown-yellow solid, which was recrystallised to give a yellow microcrystalline solid. The FAB mass spectrum of this complex exhibited peaks at *m/z* 1153, 1008, 844 and 676 (based on ^{106}Pd), which correspond to $([Pd_2L][PF_6] + 166 + 166)^+$, $([Pd_2L] + 166 + 166)^+$, $([Pd_2L] + 166)^+$ and $[Pd_2L]^+$. The presence of 'echoes' at 166 mass units higher than the base peak is a phenomenon we have observed before in FAB mass spectra of complexes containing acetate ions in a 3-nitrobenzyl alcohol matrix.[22] We believe it is due to displacement of nitrite by acetate, giving 3-acetoxybenzyl alcohol, with a molecular mass of 166. These results suggest a core stoichiometry of $[Pd_2L]^{4+}$, with a non-helical binuclear structure. This is supported by the partial elemental analysis, which is consistent with the formulation $[Pd_2L(O_2CMe)_2][PF_6]_2$. The ^1H NMR spectrum of an acetonitrile solution of this complex clearly shows ten proton environments in the aromatic region, indicating that the complex must be symmetrical, and also a singlet at δ 1.41 (intensity 6 H) assigned to acetate groups co-ordinated to the palladium centres. The acetate stretches in the vibrational spectrum are observed at 1366 and 1570 cm^{-1} and are characteristic of unidentate co-ordination of the carboxylate.[23]

The most likely structure of $[Pd_2L(O_2CMe)_2][PF_6]_2$ consistent with these observations is shown in Fig. 10. Each metal ion is in a distorted square-planar environment co-ordinated by a 'terpyridyl' fragment of L and a unidentate acetate ion. There could be a large and variable twist about the interannular C–C bond between rings C and D to minimise any unfavourable steric or electrostatic interactions between the two metal centres. The compound may be regarded as a binuclear analogue of complex cations such as $[Pd(terpy)Cl]^+$ or $[Pd(terpy)(O_2CMe)]^+$. It is interesting to compare this proposed structure with the structure of $[Pd_2(qpy)_2][PF_6]_4$,[3] in which there is no convenient complementarity between the metal ions and the ligand, and the result is an unexpected binuclear double helical structure in which each palladium(II) ion is found in a distorted five-co-ordinate environment.

In conclusion, L is a structurally very versatile ligand, capable of supporting a wide variety of complex stoichiometries and geometries. Like its smaller analogue qpy, it allows the formation of binuclear double helical complexes with several metal ions, in addition to the formation of a new trinuclear double helical ligand array. The electrochemistry and spectrochemistry of these polynuclear species is rich and interesting. We are currently further investigating the co-ordination chemistry of this ligand, and probing the features which control the formation of double helical ligand arrays.

Acknowledgements

We thank Dr. Jennifer Nutkins for assistance in recording FAB mass spectra, and the SERC for the award of a studentship (to M. D. W.) and partial funding towards the costs of a diffractometer (D. A. T.).

References

1 J. F. Stoddart, *Nature (London)*, 1988, **334**, 10; J. Libman, Y. Tor and A. Stanzer, *J. Am. Chem. Soc.*, 1987, **109**, 5880; G. Stuckmeier, U. Thewalt and J.-H. Furhop, *J. Am. Chem. Soc.*, 1976, **98**, 278; A. J. Blake, C. O. Dietrich-Buchecker, T. I. Hyde, J.-P. Sauvage and M. Schröder, *J. Chem. Soc., Chem. Commun.*, 1989, 1633 and refs. therein; C. O. Dietrich-Buchecker and J.-P. Sauvage, *Angew. Chem., Int. Ed. Engl.*, 1989, **28**, 189 and refs. therein.

2 J.-Y. Ortholand, A. M. Z. Slawin, N. Spencer, J. F. Stoddart and D. J. Williams, *Angew. Chem., Int. Ed. Engl.*, 1989, **28**, 1394; P. R. Ashton, T. T. Goodnow, A. E. Kaifer, M. V. Reddington, A. M. Z. Slawin, N. Spencer, J. F. Stoddart, C. Vicent and D. J. Williams, *Angew. Chem., Int. Ed. Engl.*, 1989, **28**, 1396.

3 E. C. Constable, M. G. B. Drew and M. D. Ward, *J. Chem. Soc., Chem. Commun.*, 1987, 1600; E. C. Constable and J. M. Holmes, *Inorg. Chim. Acta*, 1987, **126**, 187; M. Barley, E. C. Constable, S. A. Corr, M. G. B. Drew, R. C. S. McQueen, J. C. Nutkins and M. D. Ward, *J. Chem. Soc., Dalton Trans.*, 1988, 2655; E. C. Constable, M. G. B. Drew, G. Forsyth and M. D. Ward, *J. Chem. Soc., Chem. Commun.*, 1988, 1450; E. C. Constable, M. G. B. Drew, G. Forsyth and M. D. Ward, *Polyhedron*, 1989, **8**, 2551; C. J. Cathey, E. C. Constable, M. J. Hannon, D. A. Tocher and M. D. Ward, *J. Chem. Soc., Chem. Commun.*, 1990, 621; E. C. Constable, S. M. Elder, J. A. Healy, M. D. Ward and D. A. Tocher, *J. Am. Chem. Soc.*, 1990, **112**, 4590; E. C. Constable, J. M. Holmes and P. R. Raithby, *Polyhedron*, 1991, **10**, 127; E. C. Constable, *Nature (London)*, 1990, **346**, 314; E. C. Constable, S. M. Elder, J. A. Healy and D. A. Tocher, *J. Chem. Soc., Dalton Trans.*, 1990, 1010.

4 E. C. Constable, M. D. Ward and D. A. Tocher, *J. Am. Chem. Soc.*, 1990, **112**, 1256.

5 J.-M. Lehn and A. Rigault, *Angew. Chem., Int. Ed. Engl.*, 1988, **27**, 1095; J.-M. Lehn, *Angew. Chem., Int. Ed. Engl.*, 1988, **27**, 89; J.-M. Lehn, A. Rigault, J. Siegel, J. Harrowfield, B. Chevrier and D. Moras, *Proc. Natl. Acad. Sci. USA*, 1987, **84**, 2565; J.-M. Lehn, J.-P. Sauvage, J. Simon, R. Ziessel, C. Piccini-Leopardi, G. Germain, J.-P. Declercq and M. Van Meersche, *Nouv. J. Chim.*, 1983, **7**, 413; J.-P. Gisselbrecht, M. Goss, J.-M. Lehn, J.-P. Sauvage, R. Ziessel, C. Piccini-Leopardi, J. M. Arrieta, G. Germain and M. Van Meersche, *Nouv. J. Chim.*, 1984, **8**, 661; G. Struckmeier, U. Thewalt and J.-H. Furhop, *J. Am. Chem. Soc.*, 1976, **98**, 278; B. Lippert, *Nachr. Chem. Tech. Lab.*, 1990, **38**, 186; U. Koert, M. M. Harding and J.-M. Lehn, *Nature (London)*, 1990, **346**, 339; J. F. Modder, G. van Koten, K. Vrieze and A. L. Spek, *Angew. Chem., Int. Ed. Engl.*, 1989, **28**, 1698.

6 E. C. Constable, *Metals and Ligand Reactivity*, Ellis Horwood, Chichester, 1990.

7 J. E. Parks, B. E. Wagner and R. H. Holm, *J. Organomet. Chem.*, 1973, **56**, 53.

8 D. W. Adamson, *J. Chem. Soc.*, 1949, S144; R. R. Ison, F. M. Franks and K. S. Soh, *J. Pharm. Pharmacol.*, 1973, **25**, 887; E. C. Constable, S. Corr and M. D. Ward, *Inorg. Chim. Acta*, 1988, **141**, 201.

9 G. J. Kubas, *Inorg. Synth.*, 1976, **19**, 90.

10 G. Sheldrick, SHELXTL +, University of Göttingen, 1986.
11 F. Krohnke, *Synthesis*, 1976, 1.
12 F. H. Burstall, *J. Chem. Soc.*, 1938, 1662.
13 M. C. Hughes, D. J. Macero and J. M. Rao, *Inorg. Chim. Acta*, 1981, **49**, 241.
14 E. C. Constable, *Adv. Inorg. Chem. Radiochem.*, 1986, **30**, 69.
15 M. M. Morrison and D. T. Sawyer, *Inorg. Chem.*, 1978, **17**, 333.
16 D. M. L. Goodgame and G. A. Leach, *J. Chem. Soc., Dalton Trans.*, 1978, 1705.
17 A. Bencini and D. Gatteschi, *Transition Met. Chem.*, 1982, **8**, 1.
18 S. A. Cotton and J. F. Gibson, *J. Chem. Soc. A*, 1970, 2105.
19 M. Cox, B. W. Fitzsimmons, A. W. Smith, L. F. Larkworthy and K. A. Rogers, *J. Chem. Soc. A*, 1971, 2158.
20 E. C. Constable and M. D. Ward, unpublished work.
21 W. Clegg and P. J. Wheatley, *J. Chem. Soc., Dalton Trans.*, 1973, 90.
22 E. C. Constable and M. D. Ward, *J. Chem. Soc., Dalton Trans.*, 1990, 1405.
23 K. Nakamoto, *Infra-red and Raman Spectra of Inorganic and Coordination Compounds*, 3rd edn. Wiley, New York, 1978.

Received 28*th November* 1990; *Paper* 0/05369D